Upcycling of Polystyrene Waste to Poly(Ionic Liquid) Materials

Zahra Sekhavat Pour, Pravin S. Shinde & Jason E. Bara*

Department of Chemical & Biological Engineering, University of Alabama, Tuscaloosa, AL USA 35487-0203

(*) Corresponding author's email address: jbara@eng.ua.edu

Abstract:

The C-H functionalization of commodity polymers could be a promising approach for upcycling plastic waste into advanced materials, which can alter the properties of the original materials through the introduction of different functionalities onto the existing backbone structures. In this study, waste polystyrene (PS) was modified by Friedel-Crafts acylation using 4-chlorobutyryl chloride (4-CBC) followed by reaction with N-alkylimidazoles to form cationic polyelectrolytes. These methods provide access to what are essentially poly(ionic liquid) (poly(IL)) materials with properties that are distinctly different from those of the PS from which they were formed. In one notable example, the glass transition temperature (T_g) of imidazolium-functionalized PS was ~16 ^oC, which is a nearly 90 °C reduction from PS. This is also evidenced by macroscopic mechanical properties where the poly(IL) product is highly elastic in stark contrast to brittle PS. Moreover, the resulting ionomers showed self-healing behaviors in the presence of a "free" IL further contributing to the utility of the materials. The methods in this work can open opportunities to utilize waste PS to obtain a vast array of poly(IL) materials with highly tailored structures and properties.

Keywords: Upcycling, Polymer Functionalization, Friedel-Crafts Acylation, Polystyrene, Ionic Liquids

TOC Graphic

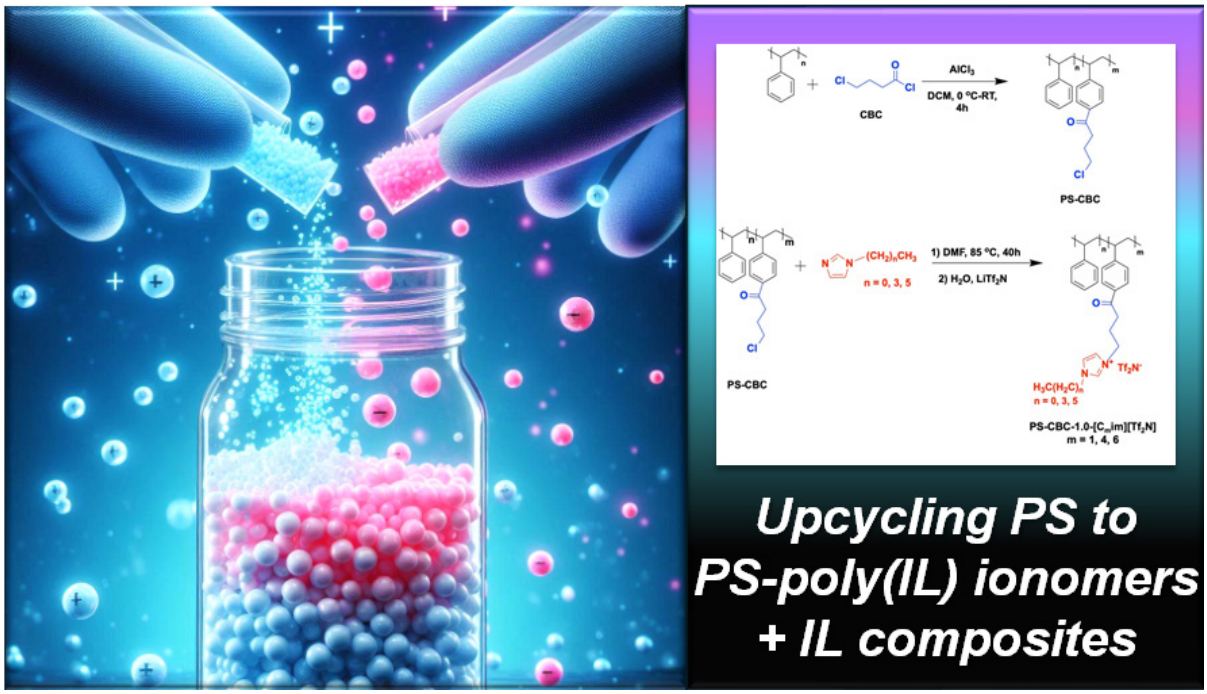
CBC
AlCl3
DCM, 0 °C-RT, 4h
PS-CBC
1) DMF, 85 °C, 40h
2) H2O, LiTf2N
n = 0, 3, 5
PS-CBC
PS-CBC-1.0-[Cnim][Tf2N]
m = 1, 4, 6
Upcycling PS to PS-poly(IL) ionomers + IL composites

1. Introduction

Polystyrene (PS) is an essential plastic, with a worldwide production exceeding 25 million tonnes (Mt) annually [1]. It is lightweight, optically clear, insulating, and easy to process (e.g., molding, extrusion, foaming). However, the ubiquity of PS in common disposable items, such as food containers, packaging materials, and insulation, has given rise to a significant environmental challenge, particularly in terms of proper disposal and recycling. Traditional mechanical recycling methods for PS often face limitations due to contaminated residues in containers, low bulk density, presence of additives, and constraints in sorting techniques leading to the production of downcycled materials, characterized by reduced quality and/or utility [2]. Hence, in the United States, the recycling rate for PS remains < 1% [3]. This challenge underscores the need for diverse and innovative approaches to address the large environmental impact of PS by using it as a low-cost starting material for more valuable polymers.

The concept of upcycling has emerged as a promising solution to help mitigate waste plastic, involving the synthesis of more valuable products, including polymers, small molecules, or materials through "depolymerization-repolymerization" or "polymer functionalization"; therefore, it is seen as a complement to mechanical recycling methods. Although still in the early stages of development, these promising alternatives have the potential to enhance the value and expand the range of applications for waste PS [4]. Polymer functionalization, also called post-polymerization modification, is a common way to tailor the characteristics of commodity and specialty plastics. Unlike the optimization of a new polymerization process, this strategy leverages the existing high-volume and economically viable post-consumer plastics waste to explore innovative materials [5]. The introduction of reactive functional groups, such as amine ($-NH_2$), alcohol (-OH), and carbonyl (>C=O), onto waste PS can have great utility since this feature not

only enhances reactivity or introduces specific properties, but also can mitigate plastic waste, conserve resources, and contribute to energy savings.

Among commodity vinyl polymers (i.e., polyethylene (PE), polypropylene (PP), and poly(vinyl chloride) (PVC)), PS stands out as the most easily modifiable due to the presence of pendant benzene rings on each repeat unit. The modification of aromatic polymers including PS can be achieved through various methods, and the choice of method depends on the specific properties and applications desired [6]. PS is naturally prone to electrophilic substitution, and it has been widely used to introduce chloromethyl groups onto PS [7-10]. Although it constitutes a highly useful functional group for further chemical reactions or modifications, in most cases, the extremely toxic and highly volatile chloromethyl methyl ether, along with a Lewis acid, must be employed for chloromethylation of PS [11, 12]. Difficulties in controlling the degree of chloromethylation, as well as issues related to crosslinking and the insertion of only a short -CH_2- linkage between the polymer backbone and chloride, represent additional possible disadvantages of halomethylation [13, 14]. Similarly, Friedel–Crafts alkylation and acylation are other commonly used techniques to modify PS with alkyl or acyl halides. This modification can impart specific chemical functionalities such as acetyl [15, 16], benzoyl groups [17], naphthoyl [18], anhydrides [19, 20], and others [21, 22]. Depending on the nature of the functional group added, this modification can significantly alter the resulting polymer's reactivity, solubility, and thermal and mechanical properties compared to the PS from which it was derived.

The application of Friedel–Crafts alkylation or acylation to aromatic polymers has been associated with a considerable broadening of the molecular weight distribution (MWD). This phenomenon occurs even at low levels of functionalization, primarily due to chain scission induced by the harsh reaction conditions [5, 23]; as a result, achieving a high degree of functionalization (DF)

becomes challenging. To mitigate this issue, various strategies have been implemented. For instance, the Friedel-Crafts acylation of PS with maleic anhydride was conducted under mild conditions using ZnO as an alternative catalyst with microwave heating. The process successfully avoided PS degradation; however, the maximum DF achieved was only ~ 9% [24]. The sequence in which reagents are added in Friedel–Crafts reactions was demonstrated to be crucial in addressing crosslinking issues; modified PS using a pre-mixed solution of chloroacylating agent and $AlCl_3$ complexed with nitrobenzene as the catalyst yielded a 10% chloroacetyl functionalization without significantly broadening the MWD [9].

Polymerization of ionic liquids (ILs) with appropriate functionalities (e.g., vinyl, acrylate, styrene) appended to the cation and/or anion will form polyelectrolytes known as poly(ionic liquids) or poly(ILs). Poly(ILs) share a number of properties with ILs including ionic conductivity, thermal stability, and a non-flammable nature [25-28]. These unique characteristics make them suitable for applications in energy storage devices (batteries, supercapacitors) [29], electrochemical sensors [30], gas separation membranes[31], and conductive materials in electronic devices [32]. Over the past ~15 years, our group has designed, synthesized, and studied a range of poly(ILs) for gas separation membranes [33-36]. Some of the IL monomers used for the fabrication of these poly(IL) materials are shown in **Figure 1**. These polymers comprise imidazolium cations (with diverse side chains) linked to PS backbones that were formed through the polymerization of imidazolium ILs bearing a styrene group. These associated IL monomers were synthesized via the reaction of N-alkyl imidazoles with 4-vinylbenzyl chloride (also known as 4-chloromethylstyrene).

Figure 1: IL-based monomers used for fabrication of poly(IL) gas separation membranes in our group.

While poly(ILs) have unique properties, and styrene-functionalized IL monomers are relatively facile to synthesize, we have frequently encountered challenges with the autopolymerization of these monomers, even when stored in a dark freezer at -10 °C. As such, an alternative synthesis of poly(IL) materials directly from PS would be desirable, as it would also allow for the number average of repeat units (i.e., X_N) in the PS backbone to be determined before conversion to a poly(IL) by conventional polymer characterization methods (e.g., gel permeation chromatography (GPC)). Of course, starting from waste PS could also reduce the overall cost and improve scalability of poly(IL) materials. In our experience, determining the X_N of poly(IL) materials with polystyrene backbones produced from the bulk polymerization imidazolium-styrene monomers was restricted as they tend to highly swell rather than dissolve in polar organic solvents [37]. To achieve this objective, it is necessary to introduce reactive functional groups (e.g., chloroalkyl), onto PS which would enable conversion to poly(IL) materials. While it may be infeasible to functionalize every benzene ring pendant from a PS backbone, partial functionalization can be achieved to obtain PS-poly(IL) ionomers, with an ionomer defined as having at least 15 mol% of ionic groups pendant from the main chain [27, 38, 39].

In this work, we aimed to obtain PS-poly(IL) ionomers to circumvent challenges associated with IL monomers as well as demonstrate new upcycling chemistries. Waste PS was functionalized through Friedel-Crafts acylation via chloroacetyl chloride (CAC) and 4-chlorobutyryl chloride (4-CBC) to introduce chloroacyl groups onto PS. For 4-CBC, a high DF of ~60% was achieved, which, to the best of our knowledge, significantly outperforms other reported Friedel-Crafts acylation reactions on PS. The introduction of chloroacyl groups onto PS creates an opportunity for the subsequent modification of waste PS with various functional groups as a means of tailoring properties. Then, we functionalized the chloroacylated PS via reaction with several different N-alkylimidazoles, resulting in PS-based ionomers with markedly different mechanical and thermal properties in comparison to the PS from which they were derived.

In recent years, Self-healing materials have gained widespread attention due to the need for enhanced repairability, which helps stabilize performance and extend the lifespan of the materials. ILs are regarded as effective self-healing agents because of their excellent conductivity, high healing efficiency, and ability to operate under mild conditions. When a polymeric matrix filled with a free IL, is damaged, healing can occur through secondary interactions such as ionic interactions between two fractured surfaces [40]. Poly(ILs) possess ionic species in each repeating unit and can form abundant ionic clusters within the polymer matrix. From this perspective, poly(IL)s can facilitate ionic association that is promising for healing applications [41]. Ionic interactions in free IL or poly(IL) are stronger than other non-covalent interactions such as π–π interactions and H-bonding. They can provide unlimited adjustment of polymeric chain structures leading to reversible self-healing properties [42]. Another interesting observation in our work was that the resulting PS-based ionomers exhibit self-healing properties in the presence of free ionic

liquid, 1-butyl-3-methylimidazolium bistriflimide ([C_4C_1im][Tf_2N]) which can further contribute to material performance and properties.

2. Experimental

2.1. Materials

Waste PS was obtained from food containers purchased locally and bearing resin identification code (RIC) 6.. Thet were cut into small plastic flakes (0.5-1.0 cm), washed with deionized water and ethanol (EtOH), and dried at 60 °C in a vacuum oven overnight. Virgin PS (M_w = 190 kDa) was purchased from Scientific Polymer Products (Ontario, NY USA) and used as a basis for comparison against waste PS. Chloroacetyl chloride (CAC) (98%), 1-bromohexane (99%), and 1-bromobutane (99%) were purchased from Alfa Aesar. 4-Chlorobutyryl chloride (4-CBC) was purchased from ThermoFisher Scientific. Anhydrous aluminum chloride ($AlCl_3$) was obtained from Beantown Chemical (Hudson NH, USA). 1-methylimidazole (C_1im) was purchased from Oakwood Chemical. Lithium bistriflimide ($LiTf_2N$, 99%) was obtained from 3M (Minneapolis, MN, USA). N,N-dimethylformamide (DMF), dichloromethane (DCM), tetrahydrofuran (THF), chloroform ($CHCl_3$), and acetonitrile (ACN) were purchased from VWR (Atlanta, GA, USA). Dimethyl sulfoxide (DMSO) was obtained from Gaylord Chemical Company (Tuscaloosa, AL USA).

2.2. Characterization

^{1}H NMR data were collected using a 500MHz Bruker Avance instrument (Billerica, MA, USA). FTIR data were obtained using a Perkin Elmer Spectrum Two ATR-FTIR instrument (Waltham, MA, USA). Quantitative FTIR analysis was conducted using absorbance at a specific wavenumber in accordance with the Lambert-Beer law. Calibration curves were prepared by mixing $LiTf_2N$ with KBr in different weight ratios. The peak at 1055 cm^{-1} was used as a reference

to quantify the Tf_2N^- content in the polymer samples [43]. The thermal stabilities of waste polystyrene (PS) and its derivatives were observed by conducting thermogravimetric analysis (TGA) using a SETARAM Labsys Evo thermal analyzer (KEP Technologies, TX, USA). To perform the TGA measurements, an appropriate amount of PS sample was packed in a high-purity cylindrical alumina (Al_2O_3) pan and heated from 25 to 600 °C at a ramp rate of 10 °C min^{-1} under a constant flow rate (10 mL min^{-1}) of ultra-high purity argon (Ar) gas (UHP300, Airgas). The glass transition temperatures (T_g) of the polymers were observed by differential scanning calorimetry (DSC) (TA Instruments DSC Q20, New Castle, DE, USA) from -40 to 180 ºC with a scan rate of 10 ºC min^{-1} under N_2 atmosphere. The heating and cooling cycles were repeated at least three times to obtain reliable and reproducible DSC results.

The number-average molecular weight (M_n), weight-average molecular weight (M_w), and polydispersity index (PDI = M_w/M_n) of the waste PS samples were determined by gel-permeation chromatography (GPC) analysis using EcoSEC Elite® GPC Autosampler System equipped with a refractive index (RI) detector (Model: HLC-8420GPC by Tosoh Bioscience, Tokyo, Japan), two in-series TSKgel Alpha-M GPC columns (7.8 mm × 30 cm × 13 um) at an operating temperature of 40 °C and an eluent flow rate of 0.5 mL min^{-1} using THF as the mobile phase. PS standards were used for calibration. The films derived from PS and PS-poly(IL) ionomers were prepared using a Carver hot-press (model 4386) at a set temperature of 180 ºC. Each sample (~2 g) was placed between two sheets of parchment paper and then centered on the lower plate of the hot-press. Subsequently, the hot-press was elevated to apply a pressure of 1500 psi, maintained under these conditions for 2 min. After releasing the pressure, the sandwiched film was removed, allowed to cool to room temperature, and peeled from the parchment paper. The thicknesses of the defect-free films produced under these conditions were within the range of 150-350 μm. Tensile testing

was conducted utilizing a compact table-top electromechanical-driven single-column load-frame universal testing machine (Test Resources Inc, Shakopee, MN, USA) equipped with a 1.1 kN load cell capacity and a speed range of 0.01 to 30 in/min controlled by Newton software. The mechanical properties of the specimens were assessed at a controlled environment of 21 ± 2 °C under ASTM D 638 standards. Three specimens were tested for each sample.

The ion exchange capacity (IEC) of PS-poly(IL) ionomers with chloride anion was determined using Volhard's method. Samples of a defined weight were soaked in 25 mL of 0.5 M $NaNO_3$ solution for 48 hours, followed by filtration and washing with water. A specific amount of 0.01 M $AgNO_3$ solution was then added, leading to the precipitation of AgCl, which was subsequently filtered. The filtrate, acidified with 1 M HNO_3, was titrated with 0.01 M KSCN in the presence of Fe(III) ions as an indicator. The IEC value was calculated using the Eqn 1:

$$IEC_{exp}\ (mmol/g) = \frac{(V_{AgNO_3} \times C_{AgNO_3}) - (V_{KSCN} \times C_{KSCN})}{m_{dry}} \quad \textbf{(1)}$$

where V and C are the volume (mL) and the concentration of $AgNO_3$ and KSCN solution (M) used in the titration and m_{dry} (g) is the mass of the dry sample.

The theoretical IEC (IEC_{theo}) was calculated based on the assumption of complete quaternization using the Eqn 2:

$$IEC_{theo}\ (mmol/g) = \frac{10 \times DF}{M_{repeat\ unit}} \quad \textbf{(2)}$$

where $DF\ (\%)$ and $M_{repeat\ unit}$ are the degree of functionalization and the average molecular weight of a repeat unit, respectively [44].

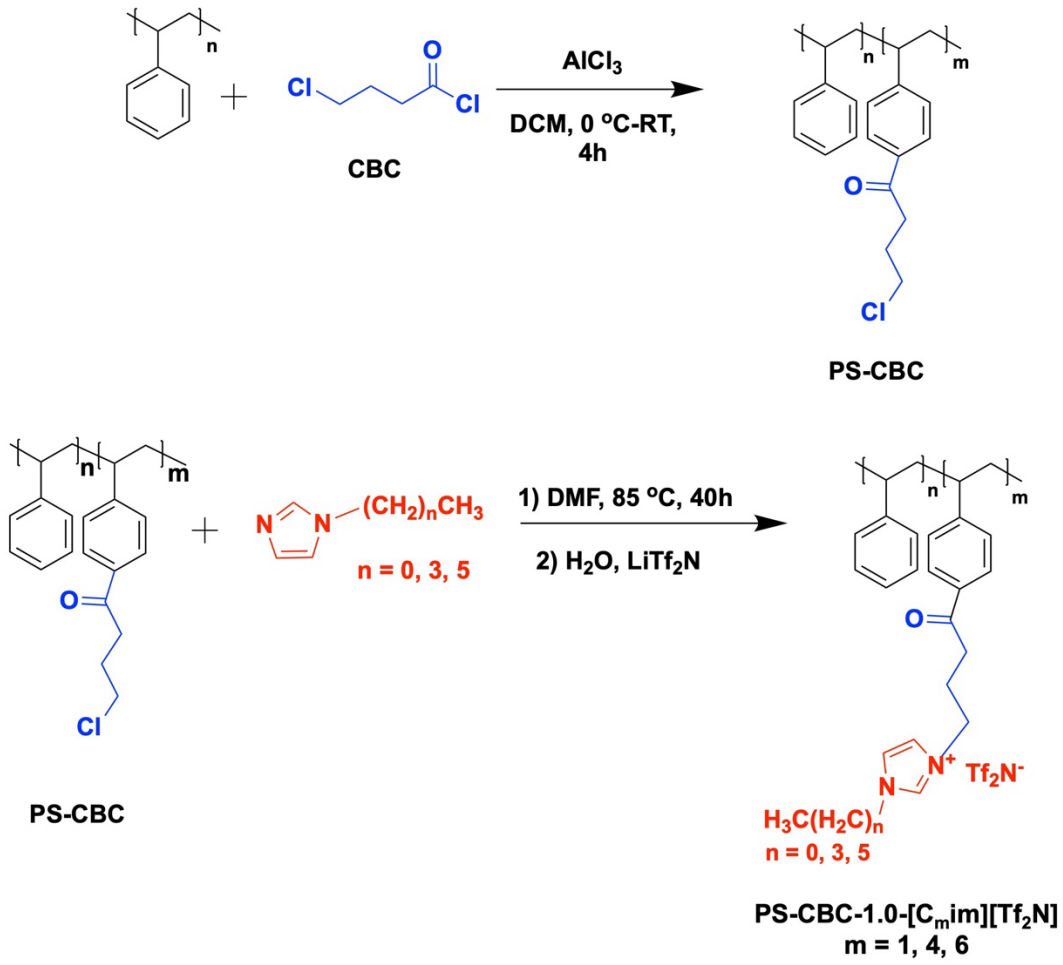

Figure 2: Synthetic procedure for PS-poly(IL) ionomers via Friedel-Crafts acylation of waste PS, followed by quaternization and ion exchange

2.3 Synthesis

2.3.1 Friedel-Crafts Acylation of waste PS

Acylation of waste PS was carried out using CAC or 4-CBC as acylation agents, and $AlCl_3$ as the Lewis acid catalyst, as depicted in **Figure 2.** When using 4-CBC, a solution of waste PS (2.00 g, 19.2 mmol styrene repeating units) in 40 mL dried DCM was prepared. $AlCl_3$ (1.28 g, 9.6 mmol) and 4-CBC (1.36g, 9.6 mmol) were mixed in the presence of 15 mL DCM, and the resulting light-yellow solution was added to the polymer solution dropwise at 0 ºC and stirred for 1 h. The

solution was stirred at room temperature for another 3 h and then precipitated in MeOH acidified with HCl. The resulting polymer (PS-CBC-0.5) was purified by dissolving in THF and reprecipitating in MeOH twice and then dried at room temperature under a vacuum for 48 h (Yield: 2.72 g). The same reaction was carried out for an equimolar mixture of 4-CBC and $AlCl_3$ catalyst, corresponding to the number of styrene repeating units in the polymer to obtain PS-CBC-1.0 (Yield: 3.17 g). The same approach was used when CAC was used as an acylation agent. When using 0.5 eq of CAC (PS-CAC-0.5), a gel was obtained which was soluble in DCM, DMF, and THF after purification. The use of 1.0 eq of CAC led to the formation of a crosslinked, insoluble polymer.

2.3.2 Synthesis of 1-Butylimidazole and 1-Hexylimidazole

N-alkylimidazoles were synthesized according to a previously reported procedure [45]. Imidazole (235 mmol) and potassium hydroxide (KOH, 235 mmol) were dissolved in 80 mL DMSO in a 250 mL round bottom flask at 50 °C. Then, 1-bromobutane or 1-bromohexane (235 mmol) was added dropwise. The mixture was stirred at 60 °C overnight and then allowed to cool to ambient temperature. Then, 200 mL of deionized water was added to the resulting mixture followed by extraction with $CHCl_3$. The organic layer was washed with brine solution and then with deionized water twice. It was dried over anhydrous $MgSO_4$ before filtration. The solvent was removed via rotary evaporation, and the excess solvent was removed in vacuo (Yield: 85% for 1-butylimidazole (C_4im) and 83% for 1-hexylimidazole (C_6im)). The ^{1}H NMR spectra of the resulting samples are shown in **Figure S1**.

2.3.3 Synthesis of imidazolium-functionalized PS

Waste PS modified with 4-CBC underwent additional functionalization through the incorporation of imidazolium cations, by using C_1im, C_4im, or C_6im. For C_1im functionalization,

a solution of PS-CBC-1.0 (2.00 g) in 40 mL DMF was prepared, and ~6 eq (4.45 g, 54.20 mmol) of C_1im was added, followed by the addition of KI (0.05 eq) as a catalyst to facilitate the Menshutkin reaction. The solution was stirred at 85 ℃ for 40 h. The product was precipitated in a beaker containing a solution of $LiTf_2N$ (15.56 g, 54.2 mmol) in 15 mL of deionized water. The mixture was stirred at room temperature overnight for the completion of anion exchange. The product was then filtered and washed with water several times and dried in a vacuum oven at 45 ℃ for 48 h. A similar procedure was used for functionalization with C_4im and C_6im; the resulting polymers were washed with MeOH/water (3:1) several times before drying.

2.3.4. Synthesis of 1-butyl-3-methylimidazolium bistriflimide ionic liquid

1-butyl-3-methylimidazolium bistriflimide ($[C_4C_1im][Tf_2N]$), used as a "free" IL for composite preparation, was prepared according to our previously reported protocol [46, 47]. Briefly, C_1im (15.02 g, 183 mmol) was dissolved in ACN (30 mL) in a 250 mL round-bottom flask. 1-chlorobutane (20.27g, 219 mmol) was added, and the reaction was refluxed while stirring for 16 h. After the reaction was cooled to room temperature, it was poured into ethyl acetate (EtOAc, 300 mL) which caused the imidazolium chloride salt to precipitate while extracting unreacted reactants. The resulting viscous liquid was added to 150 mL of deionized water, followed by adding $LiTf_2N$ (62.87g, 219 mmol) and stirring for 2 h at room temperature. The oil phase was extracted by DCM and then washed with deionized water (5 × 150 ml) and dried over anhydrous $MgSO_4$. After removing the solvent by rotary evaporation, the product was dried overnight at 65 °C under vacuum to yield $[C_4C_1im][Tf_2N]$, as a clear, colorless oil (Yield: 61.38g, 80%). The ^{1}H NMR spectrum of the resulting IL is shown in **Figure S2**.

3. RESULTS AND DISCUSSION

3.1. Synthesis of waste PS-based ionomers

Friedel-Crafts acylation is one of the most widely used methods to introduce functionality onto aromatic polymers including PS. Nevertheless, the harsh conditions generally used in this reaction may induce chain scission, consequently altering the molecular weight of the PS and broadening its MWD. Thus, to achieve a high degree of functionalization, it is necessary to implement milder reaction conditions. In Friedel-Crafts acylation reactions, the method of addition of reactants and the ratio of catalyst-to-acylating reagent play a crucial role [9, 48]. The Bouveault addition procedure involves the addition of an acylation reagent to a premixed solution of Lewis acid (e.g., $AlCl_3$) and polymer whereas in the Elbs addition procedure, the catalyst is added as the last component [49, 50]. In both methods, the ratio of catalyst to acylating reagent changes continuously based on how fast the final component is added and the rate at which acylation occurs. This can lead to early crosslinking, lower DF, and the lack of reproducibility of such reactions. However, in the Perrier procedure, a pre-mixed solution of Lewis acid catalyst and acylation reagent is added to the polymer solution, ensuring a consistent catalyst-to-acylation reagent ratio throughout the entire reaction [9]. In this study, the Perrier procedure was used for the addition of $AlCl_3$ and CAC or 4-CBC to waste polymer solution leading to not only milder reaction conditions but also achieving high DF up to around 60%. Chloroacylated PS underwent subsequent functionalization with N-alkylimidazoles, followed by ion exchange to Tf_2N anions (**Figure 2**).

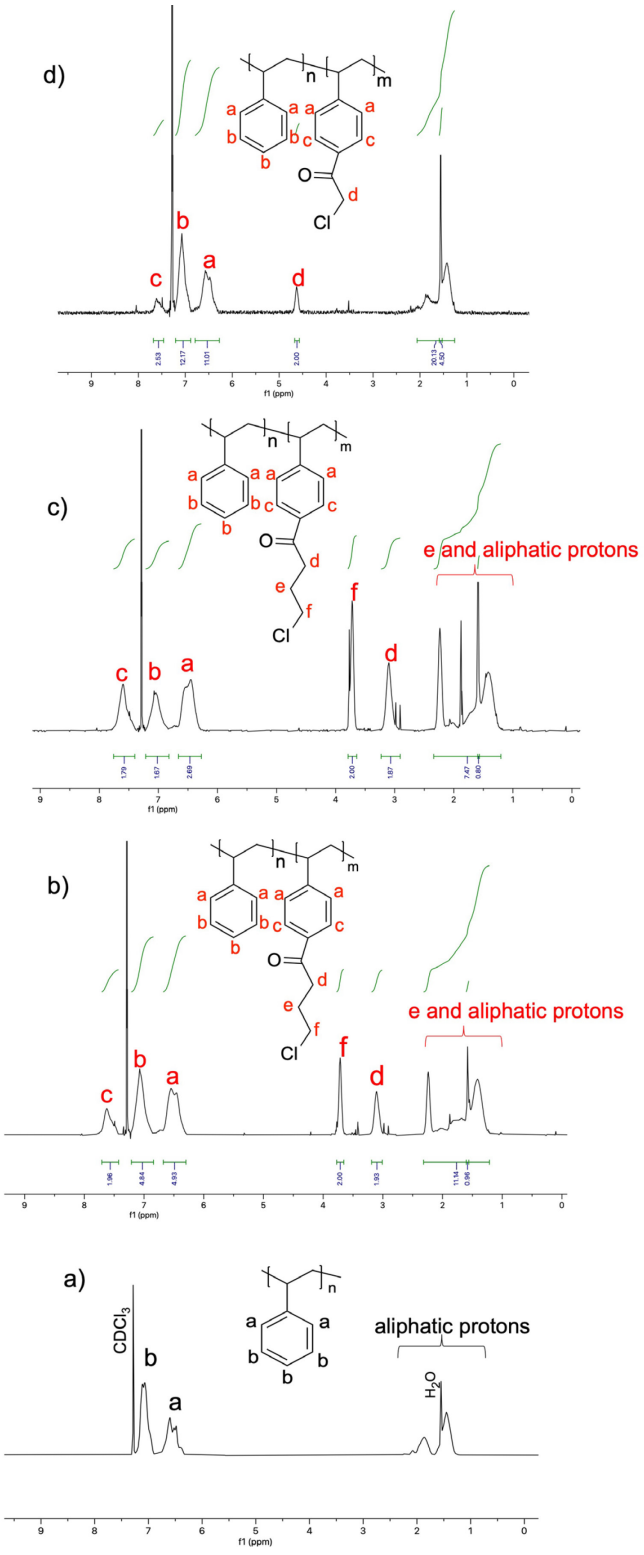

Figure 3: ^{1}H-NMR of waste a) PS, b) PS-CBC-0.5, c) PS-CBC-1.0 d) PS-CAC-0.5

Table 1: Effect of catalyst and acid chloride amount on DF, molecular weight, and polydispersity of waste PS.

Sample	PS: $AlCl_3$: 4-CBC (eq)	DF (%)		M_n [(c)] (kDa)	M_w [(d)] (kDa)	PDI [(e)]
		^{1}H NMR [(a)]	Weight gain [(b)]			
Waste PS	-	-	-	75.7	174.7	2.31
PS-CAC-0.5	1:0.5:0.5	19	22	-	-	-
PS-CBC-0.5	1:0.5:0.5	37	35	117.9	309.8	2.63
PS-CBC-1.0	1:1:1	64	57	151.5	462.8	3.06

(a) Degree of functionalization of PS rings in mol % calculated from ^{1}H NMR, (b) from weight gain, (c) M_n: Number-average molecular weight, (d) M_w: Weight-average molecular weight, and (e) PDI: Polydispersity Index (M_w/M_n)

3.2. ^{1}H NMR Analysis

Figure 3 shows the ^{1}H NMR spectra of waste PS, PS-CAC, and PS-CBC samples obtained from Friedel–Crafts acylation of waste PS. The characteristic aromatic hydrogen (Ar-H) atoms of PS are seen as two broad signals at 7.1 ppm and 6.5 ppm. The aliphatic CH_2 and CH proton signals of the PS backbone appeared at 2.2-1.3 ppm.

After the Friedel-Crafts acylation using 4-CBC, distinct peaks at 3.1, 3.8, and 7.6 ppm emerged, corresponding to the methylene group connected to the carbonyl (d), the chloromethyl (f), and the aromatic protons ortho to the carbonyl group (c), respectively (**Figure 3b**). These peaks exhibited enhanced sharpness when utilizing 1.0 equivalent of $AlCl_3$ and 4-CBC (**Figure 3c**). The DF for the styrene units obtained from both ^{1}H NMR and weight gains are summarized in **Table 1**. DF was determined using ^{1}H NMR by calculating the ratios of terminal -CH_2-Cl protons to the intensity of the aliphatic (-CH_2-CH(Ph)-) protons of the PS backbone. NMR analysis revealed that roughly 37% of the polymer's styrene units underwent acylation in PS-CBC-0.5 which is consistent with the DF calculated through weight gain. **Table 1** also shows the number-average molecular weight (M_n), weight-average molecular weight (M_w), and polydispersity index (PDI) of the waste

PS before and after acylation with 4-CBC determined with GPC. This analysis indicated M_n, M_w, and PDI were increased in this resulting polymer (PS-CBC-0.5), which is slightly broader than that of the starting waste PS (PDI = 2.3).

The DF values obtained through weight gains align with the results obtained from NMR analysis, providing consistent findings (**Table 1**). An increase in both 4-CBC and $AlCl_3$ amounts led to a significant enhancement of DF, approximately by 25%, reaching a value of 64%. A PDI value of 3.0 was measured for PS-CBC-1.0 which is due to the broadening of PS molecular weight in Friedel-Crafts acylation reaction. Despite this, the polymer is still soluble and can be used for further modification. Virgin PS with M_w of 190 kDa was used as a model in this reaction, and similar results were achieved when 4-CBC was used as an acylating agent (**Figure S3)**.

The ^{1}H NMR spectra of PS functionalized with CAC exhibit distinctive peaks at 4.7 ppm and 7.6 ppm, attributed to the chloroacetyl protons and the aromatic protons ortho to the chloroacetyl group, respectively (**Figure 3d**). The DF for the PS-CAC-0.5 sample was determined to be 19% which is significantly lower than that of the PS-CBC-0.5 sample (37%). It seems the reactivity of the acylation agent plays a crucial role in determining the degree of acylation in the Friedel-Crafts reaction. Experimentally, only the PS-CAC-0.5 sample was successfully synthesized. A higher concentration of CAC and catalyst (1 eq) in this reaction resulted in a crosslinked insoluble gel, highlighting that CAC is more reactive than 4-CBC. Due to the high reactivity of CAC, both acylation and alkylation occur simultaneously, resulting in polystyrene crosslinking. This higher reactivity of CAC is attributed to its acetyl chloride functional group, known for its high electrophilicity. In contrast, the presence of $-CH_2-$ spacers between the acid chloride and terminal $-CH_2-Cl$ group in the 4-CBC chemical structure can reduce the reactivity of both groups compared to CAC in this reaction leading to an elevated DF (due to a lower tendency

to crosslink). The proposed mechanism of polystyrene crosslinking via Friedel-Crafts reaction with CAC can be seen in **Figure S4**.

^{1}H NMR spectra of the PS-poly(IL) ionomer products are shown in **Figure S5**. After the reaction of the chloromethyl groups in PS-CBC-1.0 with the imidazole compounds, a new peak (H_l) appears at 4.5-4.8 ppm, confirming successful quaternization. The characteristic imidazolium peaks at 4.2-4.4 ppm (H_j), 7.7-8.0 ppm (H_g), and a broad peak around 9.0 ppm further confirm the grafting of imidazolium onto the waste PS. The degree of quaternization (DQ, mol %) was calculated based on the ratio of the integral of peak (H_l) to phenyl hydrogens in unreacted monomer units (6.9-7.3 ppm) and can be seen in **Table S1**. Approximately half of the PS repeat units are functionalized with pendant imidazolium cations.

3.3. FTIR Analysis

Figure 4 illustrates the FTIR spectra of PS and the PS-poly(IL) ionomer products. In the spectrum of waste PS, the as-expected absorption peaks are observed at 3060 and 3026 cm^{-1}, attributed to the aromatic C-H stretching vibration absorption. Additionally, peaks at 1601, 1492, and 1452 cm^{-1} are indicative of aromatic C=C stretching vibration absorption. Notably, the presence of peaks at 755 and 695 cm^{-1} signifies C-H out-of-plane bending vibration absorption, suggesting the existence of a singular substituent in the benzene ring [51]. Following Friedel-Crafts acylation, the emergence of two distinctive peaks at 1680 cm^{-1} and 649 cm^{-1} was observed in the FTIR spectrum of PS-CBC samples. The prominent peak at 1680 cm^{-1} is attributed to the characteristic absorption of the carbonyl group of the acyl moiety; the peak at 649 cm^{-1} is ascribed to the stretching vibration absorption associated with the C-Cl bond in terminal -CH_2-Cl group. Another new peak at 1230 cm^{-1} is due to the bending vibration absorption of the C–H bonds on the benzene ring, resulting from dual substitutions at position 1 (main chain) and position 4 after

acylation reactions [52]. After the Menshutkin reaction using C_1im, C_4im, or C_6im and subsequent anion exchange using $LiTf_2N$, the appearance of distinctive peaks corresponding to the C−N vibrations of the imidazolium cation (at 1350 cm^{-1}) and the stretching vibrations associated with SO_2 and SNS moieties (at 1180 and 1055 cm^{-1}, respectively) in the $-SO_2-N-SO_2-$ groups within the anions confirm the successful formation of the newly developed imidazolium-functionalized PS [47, 53].

The DQ was determined using multiple methods to quantify the imidazolium content attached to waste PS (**Table S1**). ^1H NMR analysis of ionomers with Cl^- anion, and the weight gain of PS-CBC-1.0 after quaternization and ion exchange with Tf_2N^- were employed to calculate the DQ in the PS-poly(IL) ionomer products. DQ was also quantified via FTIR by analyzing the absorbance peak at 1055 cm^{-1} and using the obtained Tf_2N^- weight percent (W_{Tf2N}, %) in the polymers (**Table S1**). There was close agreement between the DQ values obtained from FTIR, NMR, and the observed weight gain. The DQ obtained from FTIR data in **Table S1** also reveals that approximately half of the repeat units in waste PS were functionalized with the imidazolium compounds. This table also presents the IEC values measured by titration (IEC_{exp}) and the theoretical values (IEC_{theo}) calculated based on the DF (= 64%) from NMR. For all ionomers, IEC_{exp} values were lower than the theoretical ones, likely due to incomplete quaternization of PS-CBC-1.0 and incomplete ion exchange in the heterogeneous ion exchange reaction medium.

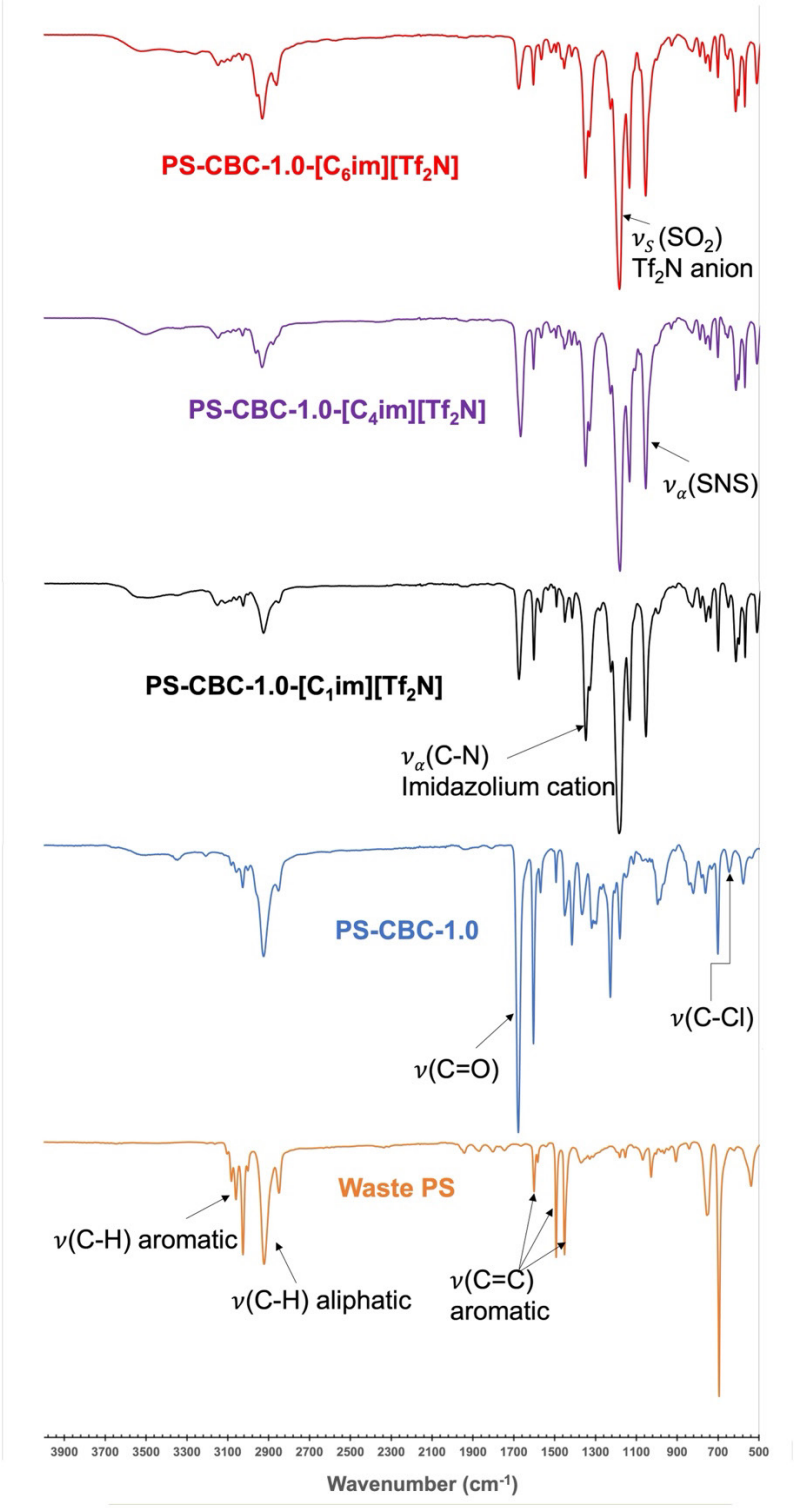

Figure 4: FTIR spectra of waste PS, PS-CBC-1.0, and its ionomer derivatives

3.4 Thermal properties

The thermal stability of waste PS and its functionalized derivatives were investigated by TGA over a range of T = 25-600 °C under an inert (Ar) atmosphere. The corresponding profiles are depicted in **Figure 5a.** TGA of PS reveals a distinctive decomposition pattern, characterized by a sharp single-step decomposition temperature at around 411 ºC. This is attributed to the primary decomposition of the main polymer backbone [54]. The stability of the phenyl group within PS is evident, with no significant changes observed below 400 °C. However, two decomposition steps were observed for the PS-CBC-1.0. There was a nearly 18% mass loss between 200 and 330 °C, corresponding to the removal of side chains (i.e. 4-CBC molecules grafted on the waste PS), followed by backbone degradation starting at ~370 ºC [55]. For PS modified with imidazolium cations, the initial slight weight loss (< 3%) before 200 °C was ascribed to the evaporation of absorbed water. Significant weight loss between 200-320 °C is attributed to the loss of imidazolium cations bound to PS and [Tf_2N] anion decomposition. Moreover, the difference in the char yields at 600 ºC between waste PS and ionomers (**Table S2**) confirms the presence of an extra organic fraction in the polymer structure. Similar behavior was observed when cross-linked chloromethylated PS was functionalized with imidazolium cations with OH^- and Cl^- counter anions [56, 57].

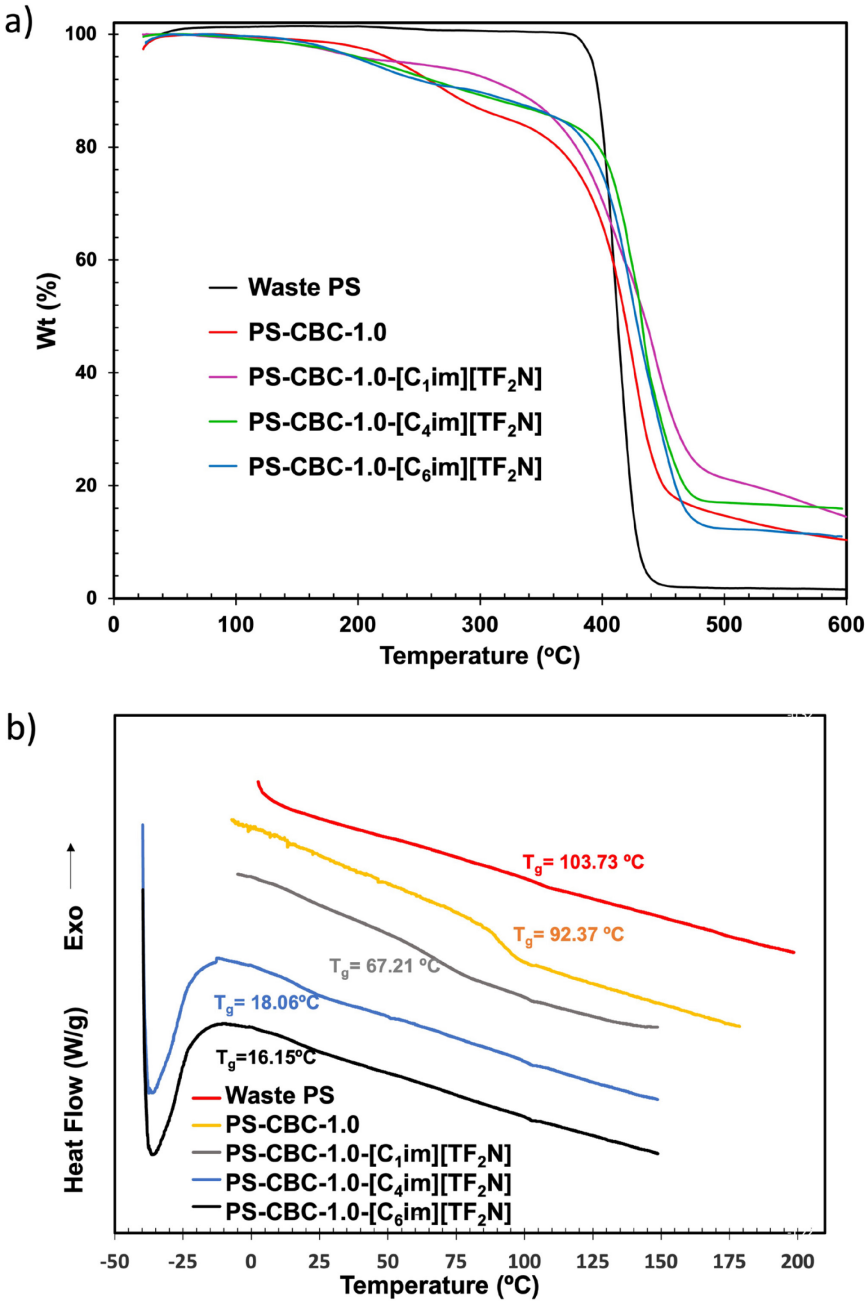

Figure 5: a) TGA and b) DSC spectra of waste PS and its ionomer derivatives.

DSC analysis was performed to investigate the changes in the glass transition temperature (T_g) of waste PS as a result of modification with the different imidazolium cations. As depicted in **Figure 5b** and **Table S2,** waste PS exhibited a T_g at ~103 °C; after Friedel-Crafts reaction with 4-

CBC, it decreased by nearly 11 °C. It seems that functional groups attached to the polymer backbone create higher free volume, preventing the close packing of polymer chains. However, the intermolecular interactions of polar chloromethyl groups prevent further changes in T_g. PS functionalization with [C_1im][Tf_2N] led to a reduction in the T_g to 67.21 °C, indicating the glassy state of this polymer at ambient temperature. The introduction of [C_4im][Tf_2N] and [C_6im][Tf_2N] had a much greater impact on T_g. DSC findings demonstrated that functionalization with [C_4im][Tf_2N] and [C_6im][Tf_2N] reduced the T_g to 18.06 and 16.15 °C respectively. This significant reduction in T_g can be attributed to the larger and flexible alkyl side groups in [C_4im]PS and [C_6im]PS, which enhance free volume and, consequently, the mobility of polymer segments. Additionally, the presence of large counter ions (Tf_2N^-) weakened ion associations and had a plasticizing effect, contributing to increased flexibility.

3.5. Mechanical Properties

The tensile strength and elongation at break of waste PS and the imidazolium-modified PS samples are depicted in **Figure 6e** and summarized in **Table S3**. Among the prepared samples, waste PS exhibited the highest tensile strength at ~23 MPa but demonstrated the least strain, indicative of its inherently brittle nature. After modification with imidazolium cations, the stress-strain curves of the modified PS are consistent with the behavior of elastic polymers. The C_1im-functionalized PS displayed a higher tensile strength compared to C_4im and C_6im-modified PS. However, its strain was limited to 26.74%. As mentioned earlier, the T_g of PS-CBC-1.0-[C_1im][TF_2N] is above room temperature, rendering it brittle under these conditions, as also illustrated by **Figure 6a**. The introduction of the free IL ([C_4C_1im][Tf_2N]) with 30 wt% to PS-CBC-1.0-[C_1im][TF_2N] resulted in a composite with improved tensile strength and notably high strain (~180%). This transparent thin film can be seen in **Figure 6b**. This enhancement can be

attributed to the IL acting as a plasticizer. They penetrate between polymer chains and interact with ionic parts of the polymer, increasing elasticity and reducing brittleness. [C_4im] PS and [C_6im] PS functionalization yielded more flexible and stretchable materials, due to their longer alkyl side chains. Transparent defect-free films of these two samples can be seen in **Figure 6c** and **d**. The elongation at break for the PS-CBC-1.0-[C_4im][Tf_2N] film increased nearly 500%. Interestingly, this modification eliminated the need for the addition of free IL as [C_4im] PS and [C_6im] PS functionalization made the polymer flexible inherently. It seems the length of the alkyl chain played a crucial role, as the [C_6im]-functionalized PS exhibited a more gel-like behavior, leading to a decrease in both tensile strength and strain. These results suggest that the modification of waste PS with [C_4im] or [C_6im] transforms its brittle nature into an elastic characteristic which could make these materials viable alternatives to our previous methods for fabricating poly(IL) and IL composite gas separation membranes [25, 34].

For gas separation membrane application, there is no universally fixed target strength/strain, as it depends on the polymer chemistry, specific application, and operating conditions. Polymers used for such membranes typically exhibit tensile strengths ranging from 1 to 100 MPa and elongations at break between 1% and 400% [58-61]. For instance, a thermal rearrangement (TR) copolymer membrane has demonstrated a high tensile strength of 95 MPa with a low strain of 3% [59], while elastic polymer membranes like urethane-rich poly(dimethylsiloxane) (PDMS) exhibit around 400% elongation at break with only 1.4 MPa tensile strength [58]. The PS-based ionomers synthesized in this work, with promising stretching ability, are expected to significantly enhance the mechanical performance of membranes by reducing susceptibility to defects compared to glassy polymer membranes for gas separation. Additionally, the incorporation of imidazolium functionality is anticipated to improve gas

selectivity although the high chain mobility in stretchable polymer membranes could result in a lower selectivity. These hypotheses will be evaluated in future research, as we aim to evaluate the gas separation performance of these materials.

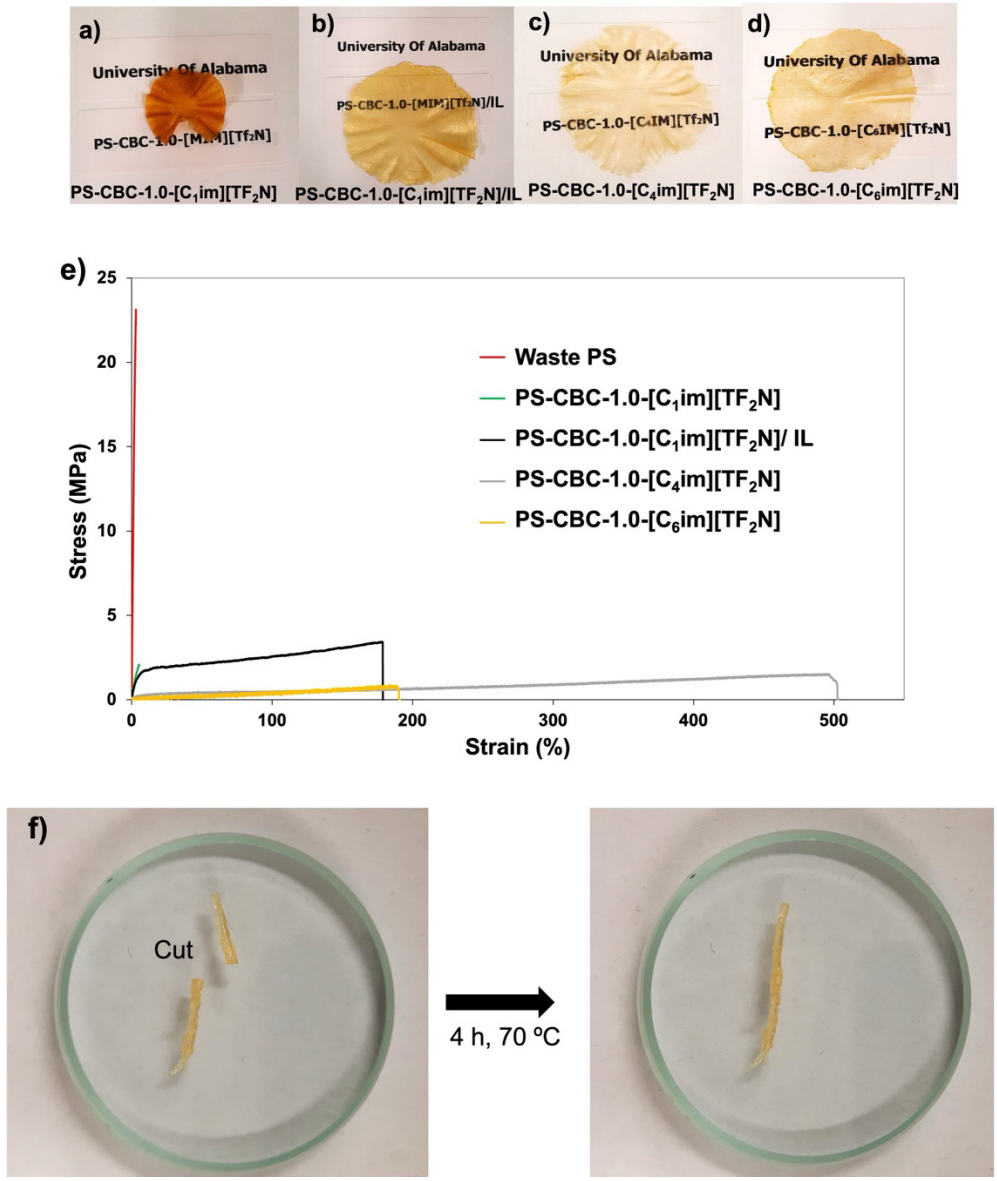

Figure 6: a-d) Photographs of hot-pressed films of PS-based ionomers: a) PS-CBC-1.0-[C_1im][Tf_2N], b) PS-CBC-1.0-[C_1im][Tf_2N]/IL composite, c) PS-CBC-1.0-[C_4im][Tf_2N] and d) PS-CBC-1.0-[C_6im][Tf_2N], and e) Stress-Strain profiles of waste PS and its ionomer derivatives. f) Self-healing property of PS-CBC-1.0-[C_1im][Tf_2N] containing 50 wt%[C_4C_1im][Tf_2N] IL before and after healing.

3.6. Self-healing Properties

The resulting films made of PS-based ionomer were examined to evaluate their potential self-healing properties. Whitley, et al. previously reported that bulk poly(ILs) that were recovered from autopolymerized imidazolium-styrene monomers displayed self-healing and shape memory behaviors [35]. Although the original PS-poly(IL) ionomers did not display self-healing characteristics (possibly because of the reduced ion concentration per styrene unit), their composites with ILs demonstrated such properties. PS-based ionomer composite containing $[C_1im][Tf_2N]$ with added 50 wt% $[C_4C_1im][Tf_2N]$ IL exhibited self-healing after maintaining at 70 °C for 4 h (**Figure 6f** and **Video S1**). The IL not only acted as a plasticizer, enhancing flexibility and mechanical properties through non-covalent interactions between polymer chains, but its electrostatic interactions also facilitated the healing of films post-breakage. The plasticizing effect of the IL is evident in the decrease of T_g, with the T_g of PS-CBC-1.0-$[C_1im][Tf_2N]$ dropping to about 8 °C after the addition of 50 wt% free IL (**Figure S6**). However, $[C_4im]$ and $[C_6im]$ modified PS composites, with a lower IL content of only 20 wt%, demonstrated immediate self-healing properties at room temperature (**Video S2**). The T_g values decreased to -1 °C and 4 °C for PS functionalized with $[C_4im][Tf_2N]$ and $[C_6im][Tf_2N]$ containing 20 wt% of free IL respectively (**Figure S6).** The reversible nature of ionic (or electrostatic) interactions of oppositely charged species in both IL and the resulting PS ionomers can facilitate self-healing by enabling the material to reconnect at damaged sites, leading to high healing efficiency. To evaluate the self-healing capacity, tensile tests were conducted on the original and healed PS-CBC-1.0-$[C_4im][Tf_2N]$/IL composites. The specimens were cut in half, rejoined without applying external stimuli, and tested after just 10 minutes, confirming their remarkable self-healing capabilities (**Figure S7**). The tensile strength ratio between the healed and original samples, defined as the healing efficiency (HE), was

84% after the first healing cycle and 56% after the second. This underscores the ability to achieve rapid and acceptable self-healing by fine-tuning the ionomer structures. Further research will be conducted in this area to explore these findings in greater detail.

4. Conclusions

This study demonstrates the possibility of transforming PS, a commodity plastic and ubiquitous waste, directly into imidazolium-functionalized ionomers which have potential applications in gas separation membranes and electrochemical energy materials. The Friedel-Crafts acylation of waste PS using 4-CBC, a less reactive acid chloride than CAC, proved efficient, yielding a high DF at around 60%. Subsequently, the chloroacylated polymer underwent further functionalization with three distinct imidazole molecules to form polymer-bound imidazolium cations, followed by anion exchange from Cl^- to the robust and hydrophobic Tf_2N^- form. The processability of these ionomers was demonstrated through the pressing of transparent defect-free films. A remarkable decrease in T_g was established upon the functionalization of PS with [C_4im] and [C_6im] cations, resulting in converting the inherent brittleness of PS to elastic properties. These findings demonstrate the influential role of the grafted ion structure on the mechanical and thermal properties of resulting PS-based ionomers. Furthermore, the self-healing properties of IL-functionalized PS containing free IL were demonstrated, suggesting new possibilities for developing more sustainable materials with enhanced durability and extended lifespan. This work underscores the possibility of efficiently upcycling PS waste through post-polymerization functionalization into building blocks for high-performance ionomers which can be tailored to form imidazolium cations (among many other possible chemical modifications).

Supporting Information

The Supporting Information is available free of charge at

https://pubs.acs.org/doi/10.1021.acsapm.XXXXXX

^{1}H NMR spectra of C_4im, C_6im, [C_4C_1im][Tf_2N], and modified PS(190 K). Proposed mechanism of polystyrene crosslinking via Friedel-Crafts reaction with CAC, ^{1}H NMR spectra of the PS-poly(IL) ionomer, T_g of the ionomer composites, Tensile stress-strain curves of the original and healed PS-CBC-1.0-[C_4im][Tf_2N]/IL(20wt%) ionomer composites for two times only after 10 min. Degree of quaternization of PS rings in mol % calculated by different methods and IEC of ionomers, Thermal properties of waste PS and its ionomer derivatives, Mechanical properties of waste PS and its ionomer derivatives. Videos showing self-healing behaviors.

Notes

The image on the left side of the TOC graphic was created by the authors using AI generative software (Microsoft Copilot). The terms of use associated with the software are being followed. All other images/photographs were fully created by the authors.

The authors declare no competing financial interest.

Acknowledgments

Partial support for this work provided by the United States Department of Energy (DE-SC0023473) and the National Science Foundation (EFMA-2029387) is gratefully acknowledged. The authors also thank Dr. Artie McKim from Gaylord Chemical Company for the donation of DMSO used in these studies.

References:

(1) Geyer, R.; Jambeck, J. R.; Law, K. L. Production, use, and fate of all plastics ever made. *Science advances* **2017**, *3* (7), e1700782.
(2) Jehanno, C.; Alty, J. W.; Roosen, M.; De Meester, S.; Dove, A. P.; Chen, E. Y.-X.; Leibfarth, F. A.; Sardon, H. Critical advances and future opportunities in upcycling commodity polymers. *Nature* **2022**, *603* (7903), 803-814.
(3) Rahimi, A.; García, J. M. Chemical recycling of waste plastics for new materials production. *Nature Reviews Chemistry* **2017**, *1* (6), 0046.
(4) Yeung, C. W.; Teo, J. Y.; Loh, X. J.; Lim, J. Y. Polyolefins and polystyrene as chemical resources for a sustainable future: challenges, advances, and prospects. *ACS Materials Letters* **2021**, *3* (12), 1660-1676.
(5) Williamson, J. B.; Lewis, S. E.; Johnson III, R. R.; Manning, I. M.; Leibfarth, F. A. C− H functionalization of commodity polymers. *Angewandte Chemie International Edition* **2019**, *58* (26), 8654-8668.
(6) Moulay, S. Functionalized polystyrene and polystyrene-containing material platforms for various applications. *Polymer-Plastics Technology and Engineering* **2018**, *57* (11), 1045-1092.
(7) Hirao, A.; Hayashi, M. Synthesis of well-defined functionalized polystyrenes with a definite number of chloromethylphenyl groups at chain ends or in chains by means of anionic living polymerization in conjunction with functional group transformation. *Macromolecules* **1999**, *32* (20), 6450-6460.
(8) Qu, J.-B.; Xu, Y.-L.; Liu, Y.; Wang, Y.; Sui, Y.; Liu, J.-G.; Wang, X. Inherently fluorescent polystyrene microspheres for coating, sensing and cellular imaging. *Colloids and Surfaces B: Biointerfaces* **2017**, *152*, 475-481.
(9) Tizpar, S.; Abbasian, M.; Taromi, F. A.; Entezami, A. A. Grafting of poly (methyl methacrylate) or polyacrylonitrile onto polystyrene using ATRP technique. *Journal of applied polymer science* **2006**, *100* (4), 2619-2627.
(10) Serhiichuk, D.; Tian, D.; Almind, M. R.; Ma, Z.; Xia, Y.; Kraglund, M. R.; Bae, C.; Jensen, J. O.; Aili, D. Carboxylated Polystyrene-b-poly (ethylene-ran-butylene)-b-polystyrene Membranes for Alkaline Water Electrolysis. *ACS Applied Energy Materials* **2024**, *7* (3), 1080-1091.
(11) Pinell, R.; Khune, G.; Khatri, N.; Manatt, S. Concerning the chloromethylation of alkylbenzenes and polystyrenes by chloromethyl methyl ether. *Tetrahedron letters* **1984**, *25* (33), 3511-3514.
(12) Golubenko, D. V.; Van der Bruggen, B.; Yaroslavtsev, A. B. Novel anion exchange membrane with low ionic resistance based on chloromethylated/quaternized-grafted polystyrene for energy efficient electromembrane processes. *Journal of Applied Polymer Science* **2020**, *137* (19), 48656.
(13) Liu, R.; Liu, M.; Wu, S.; Che, X.; Dong, J.; Yang, J. Assessing the influence of various imidazolium groups on the properties of poly (vinyl chloride) based high temperature proton exchange membranes. *European Polymer Journal* **2020**, *137*, 109948.
(14) Lu, W.; Shao, Z.-G.; Zhang, G.; Li, J.; Zhao, Y.; Yi, B. Preparation of anion exchange membranes by an efficient chloromethylation method and homogeneous quaternization/crosslinking strategy. *Solid State Ionics* **2013**, *245*, 8-18.
(15) Li, J.; Gauthier, M. A novel synthetic path to arborescent graft polystyrenes. *Macromolecules* **2001**, *34* (26), 8918-8924.

(16) Zhang, W.; Slaný, M.; Zhang, J.; Liu, Y.; Zang, Y.; Li, Y.; Chen, G. Acetylation modification of waste polystyrene and its use as a crude oil flow improver. *Polymers* **2021**, *13* (15), 2505.
(17) Chen, Y.; Tavakley, A. E.; Mathiason, T. M.; Taton, T. A. Photocrosslinked poly (vinylbenzophenone)-core micelles via mild Friedel–Crafts benzoylation of polystyrene amphiphiles. *Journal of Polymer Science Part A: Polymer Chemistry* **2006**, *44* (8), 2604-2614.
(18) Jones, A. S.; Wright, T.; Smook, M. A.; Harwood, H. J. Enhancement of the high-temperature utility of a polystyrene-b-poly (ethylene-co-butylene)-b-polystyrene block copolymer by friedel–crafts naphthoylation. *Journal of applied polymer science* **2003**, *88* (5), 1289-1295.
(19) Nair, C. R.; Manshad, P.; Ashir, A.; Athul, S. Synthesis of 3-carbonoyl acrylic acid-functionalized polystyrene and an insight in to its role in cross linking and grafting of polystyrene on to natural rubber. *European Polymer Journal* **2020**, *131*, 109688.
(20) Li, J.; Li, H.-M. Functionalization of syndiotactic polystyrene with succinic anhydride in the presence of aluminum chloride. *European polymer journal* **2005**, *41* (4), 823-829.
(21) Wu, Y.; Li, L.; Yang, W.; Feng, S.; Liu, H. Hybrid nanoporous polystyrene derived from cubic octavinylsilsesquioxane and commercial polystyrene via the Friedel–Crafts reaction. *RSC advances* **2015**, *5* (17), 12987-12993.
(22) Liu, F.; Chen, S.; Gao, Y.; Xie, Y. Synthesis and CO2 adsorption behavior of amine-functionalized porous polystyrene adsorbent. *Journal of Applied Polymer Science* **2017**, *134* (28), 45046.
(23) Nanbu, H.; Sakuma, Y.; Ishihara, Y.; Takesue, T.; Ikemura, T. Catalytic degradation of polystyrene in the presence of aluminum chloride catalyst. *Polymer degradation and stability* **1987**, *19* (1), 61-76.
(24) Coustet, M. E.; Cortizo, M. S. Functionalization of styrenic polymer through acylation and grafting under microwave energy. *Polymer journal* **2011**, *43* (3), 265-271.
(25) Bara, J. E.; Gabriel, C. J.; Hatakeyama, E. S.; Carlisle, T. K.; Lessmann, S.; Noble, R. D.; Gin, D. L. Improving CO2 selectivity in polymerized room-temperature ionic liquid gas separation membranes through incorporation of polar substituents. *Journal of Membrane Science* **2008**, *321* (1), 3-7.
(26) Kammakakam, I.; Bara, J. E.; Jackson, E. M. Dual anion–cation crosslinked poly (ionic liquid) composite membranes for enhanced CO2 separation. *ACS Applied Polymer Materials* **2020**, *2* (11), 5067-5076.
(27) Eftekhari, A.; Saito, T. Synthesis and properties of polymerized ionic liquids. *European Polymer Journal* **2017**, *90*, 245-272.
(28) Park, J. B.; Isik, M.; Park, H. J.; Jung, I. H.; Mecerreyes, D.; Hwang, D.-H. Polystyrene-block-Poly (ionic liquid) copolymers as work function modifiers in inverted organic photovoltaic cells. *ACS applied materials & interfaces* **2018**, *10* (5), 4887-4894.
(29) Hernández, G.; Işik, M.; Mantione, D.; Pendashteh, A.; Navalpotro, P.; Shanmukaraj, D.; Marcilla, R.; Mecerreyes, D. Redox-active poly (ionic liquid) s as active materials for energy storage applications. *Journal of Materials Chemistry A* **2017**, *5* (31), 16231-16240.
(30) Guterman, R.; Ambrogi, M.; Yuan, J. Harnessing Poly (ionic liquid) s for Sensing Applications. *Macromolecular Rapid Communications* **2016**, *37* (14), 1106-1115.
(31) Ravula, S.; Wise, K. W.; Shinde, P. S.; Bara, J. E. Design and Performance of Di-and Tricationic Poly (ionic liquid)+ Ionic Liquid Composite Membranes for CO2 Separation. *Macromolecules* **2023**, *56* (15), 6126-6141.

(32) Chen, M.; White, B. T.; Kasprzak, C. R.; Long, T. E. Advances in phosphonium-based ionic liquids and poly (ionic liquid) s as conductive materials. *European Polymer Journal* **2018**, *108*, 28-37.
(33) Bara, J. E.; Hatakeyama, E. S.; Gin, D. L.; Noble, R. D. Improving CO2 permeability in polymerized room-temperature ionic liquid gas separation membranes through the formation of a solid composite with a room-temperature ionic liquid. *Polymers for Advanced Technologies* **2008**, *19* (10), 1415-1420.
(34) Bara, J. E.; Noble, R. D.; Gin, D. L. Effect of "Free" cation substituent on gas separation performance of polymer− room-temperature ionic liquid composite membranes. *Industrial & engineering chemistry research* **2009**, *48* (9), 4607-4610.
(35) Whitley, J. W.; Jeffrey Horne, W.; Shannon, M. S.; Andrews, M. A.; Terrell, K. L.; Hayward, S. S.; Yue, S.; Mittenthal, M. S.; O'Harra, K. E.; Bara, J. E. Systematic Investigation of the Photopolymerization of Imidazolium-Based Ionic Liquid Styrene and Vinyl Monomers. *Journal of Polymer Science Part A: Polymer Chemistry* **2018**, *56* (20), 2364-2375.
(36) Hatakeyama, E. S.; Ju, H.; Gabriel, C. J.; Lohr, J. L.; Bara, J. E.; Noble, R. D.; Freeman, B. D.; Gin, D. L. New protein-resistant coatings for water filtration membranes based on quaternary ammonium and phosphonium polymers. *Journal of membrane science* **2009**, *330* (1-2), 104-116.
(37) Horne, W. J.; Andrews, M. A.; Terrill, K. L.; Hayward, S. S.; Marshall, J.; Belmore, K. A.; Shannon, M. S.; Bara, J. E. Poly(Ionic Liquid) Superabsorbent for Polar Organic Solvents. *ACS Applied Materials & Interfaces* **2015**, *7* (17), 8979-8983. DOI: 10.1021/acsami.5b01921.
(38) O'Harra, K. E.; Noll, D. M.; Kammakakam, I.; DeVriese, E. M.; Solis, G.; Jackson, E. M.; Bara, J. E. Designing Imidazolium Poly (amide-amide) and Poly (amide-imide) Ionenes and Their Interactions with Mono-and Tris (imidazolium) Ionic Liquids. *Polymers* **2020**, *12* (6), 1254.
(39) Demarteau, J.; O'Harra, K. E.; Bara, J. E.; Sardon, H. Valorization of Plastic Wastes for the Synthesis of Imidazolium-Based Self-Supported Elastomeric Ionenes. *ChemSusChem* **2020**, *13* (12), 3122-3126.
(40) Zhang, W.; Jiang, H.; Chang, Z.; Wu, W.; Wu, G.; Wu, R.; Li, J. Recent achievements in self-healing materials based on ionic liquids: A review. *Journal of Materials Science* **2020**, *55*, 13543-13558.
(41) Cui, J.; Nie, F.-M.; Yang, J.-X.; Pan, L.; Ma, Z.; Li, Y.-S. Novel imidazolium-based poly (ionic liquid) s with different counterions for self-healing. *Journal of Materials Chemistry A* **2017**, *5* (48), 25220-25229.
(42) Hager, M. D.; Greil, P.; Leyens, C.; Van Der Zwaag, S.; Schubert, U. S. Self-healing materials. *Advanced Materials* **2010**, *22* (47), 5424-5430.
(43) Casarano, R.; Fidale, L. C.; Lucheti, C. M.; Heinze, T.; El Seoud, O. A. Expedient, accurate methods for the determination of the degree of substitution of cellulose carboxylic esters: Application of UV–vis spectroscopy (dye solvatochromism) and FTIR. *Carbohydrate polymers* **2011**, *83* (3), 1285-1292.
(44) An, S. J.; Kim, J. E.; Yu, S.; Kim, K. J.; Kim, M.; Kim, J. H.; Lee, J. H.; Chi, W. S. Ionic Triptycene Additive-Blended Poly (2, 6-dimethyl-1, 4-phenylene oxide)-Based Anion Exchange Membranes for Water Electrolyzers. *ACS Applied Energy Materials* **2023**, *6* (17), 8929-8940.
(45) Zhao, X.; An, D.; Ye, Z. A comprehensive study on the synthesis and micellization of disymmetric gemini imidazolium surfactants. *Journal of Surfactants and Detergents* **2016**, *19*, 681-691.

(46) Kammakakam, I.; O'Harra, K. E.; Jackson, E. M.; Bara, J. E. Synthesis of imidazolium-mediated Poly (benzoxazole) Ionene and composites with ionic liquids as advanced gas separation membranes. *Polymer* **2021**, *214*, 123239.
(47) O'Harra, K. E.; Kammakakam, I.; Devriese, E. M.; Noll, D. M.; Bara, J. E.; Jackson, E. M. Synthesis and performance of 6FDA-based polyimide-ionenes and composites with ionic liquids as gas separation membranes. *Membranes* **2019**, *9* (7), 79.
(48) Olah, G. A. *Friedel-Crafts and related reactions*; Interscience Publishers, 1963.
(49) Edwards Jr, J.; McGuire, S. E.; Hignite, C. Friedel—Crafts Acylation. Positional Selectivity and Reactivity of Acylating Agents. *The Journal of Organic Chemistry* **1964**, *29* (10), 3028-3032.
(50) Titinchi, S. J.; Kamounah, F. S.; Abbo, H. S.; Hammerich, O. The synthesis of mono-and diacetyl-9H-fluorenes. Reactivity and selectivity in the Lewis acid catalyzed Friedel-Crafts acetylation of 9H-fluorene. *Arkivoc* **2008**, *13*, 91-105.
(51) Fang, J.; Xuan, Y.; Li, Q. Preparation of polystyrene spheres in different particle sizes and assembly of the PS colloidal crystals. *Science China Technological Sciences* **2010**, *53*, 3088-3093.
(52) Gao, B.; Wang, L.; Du, R.; Li, Y. Synthesis of N-butylphthalimide catalyzed by quaternary phosphonium salt-type triphase catalysts based on cross-linked polystyrene microspheres. *International Journal of Chemical Kinetics* **2011**, *43* (12), 677-686.
(53) Kammakakam, I.; Bara, J. E.; Jackson, E. M.; Lertxundi, J.; Mecerreyes, D.; Tomé, L. C. Tailored CO2-philic anionic poly (ionic liquid) composite membranes: Synthesis, characterization, and gas transport properties. *ACS Sustainable Chemistry & Engineering* **2020**, *8* (15), 5954-5965.
(54) Abate, L.; Bottino, F. A.; Cicala, G.; Chiacchio, M. A.; Ognibene, G.; Blanco, I. Polystyrene nanocomposites reinforced with novel dumbbell-shaped phenyl-POSSs: Synthesis and thermal characterization. *Polymers* **2019**, *11* (9), 1475.
(55) Dong, J.; Li, H.; Ren, X.; Che, X.; Yang, J.; Aili, D. Anion exchange membranes of bis-imidazolium cation crosslinked poly (2, 6-dimethyl-1, 4-phenylene oxide) with enhanced alkaline stability. *International Journal of Hydrogen Energy* **2019**, *44* (39), 22137-22145.
(56) Yang, W.; Li, H.; Wu, Q.; Ren, Y.; Shi, D.; Zhao, Y.; Jiao, Q. Functionalized core–shell polystyrene sphere-supported alkaline imidazolium ionic liquid: an efficient and recyclable catalyst for knoevenagel condensation. *ACS Sustainable Chemistry & Engineering* **2020**, *8* (49), 18126-18137.
(57) Kou, X.; Ma, B.; Zhang, R.; Cai, M.; Huang, Y.; Yang, Y. Properties and mechanism for selective adsorption of Au (iii) on an ionic liquid adsorbent by grafting N-methyl imidazole onto chloromethylated polystyrene beads. *RSC advances* **2020**, *10* (34), 20338-20348.
(58) Cao, P.-F.; Li, B.; Hong, T.; Xing, K.; Voylov, D. N.; Cheng, S.; Yin, P.; Kisliuk, A.; Mahurin, S. M.; Sokolov, A. P. Robust and elastic polymer membranes with tunable properties for gas separation. *ACS Applied Materials & Interfaces* **2017**, *9* (31), 26483-26491.
(59) Zhang, J.; Lu, Y.; Xiao, G.; Hou, M.; Li, L.; Wang, T. Enhanced gas separation and mechanical properties of fluorene-based thermal rearrangement copolymers. *RSC advances* **2021**, *11* (22), 13164-13174.
(60) Pournaghshband Isfahani, A.; Sadeghi, M.; Wakimoto, K.; Shrestha, B. B.; Bagheri, R.; Sivaniah, E.; Ghalei, B. Pentiptycene-based polyurethane with enhanced mechanical properties and CO2-plasticization resistance for thin film gas separation membranes. *ACS applied materials & interfaces* **2018**, *10* (20), 17366-17374.

(61) Min, H. J.; Kim, Y. J.; Kang, M.; Seo, C.-H.; Kim, J.-H.; Kim, J. H. Crystalline elastomeric block copolymer/ionic liquid membranes with enhanced mechanical strength and gas separation properties. *Journal of Membrane Science* **2022**, *660*, 120837.